Korean J. Chem. Eng., **30**(12), 2205-2212 (2013)
DOI: 10.1007/s11814-013-0168-7

pISSN: 0256-1115
eISSN: 1975-7220

An electrostatic sensor for the continuous monitoring of particulate air pollution

Panich Intra*,†, Artit Yawootti*, and Nakorn Tippayawong**

*Research Unit of Electrostatic Applications in Energy and Environment, College of Integrated Science and Technology, Rajamangala University of Technology Lanna, Chiang Mai 50220, Thailand
**Department of Mechanical Engineering, Faculty of Engineering, Chiang Mai University, Chiang Mai 50200, Thailand
(*Received 12 March 2013 • accepted 3 September 2013*)

Abstract−We developed and evaluated a particulate air pollution sensor for continuous monitoring of size resolved particle number, based on unipolar corona charging and electrostatic detection of charged aerosol particles. The sensor was evaluated experimentally using combustion aerosol with particle sizes in the range between approximately 50 nm and several microns, and particle number concentrations larger than 10^{10} particles/m^3. Test results were very promising. It was demonstrated that the sensor can be used in detecting particle number concentrations in the range of about 2.02×10^{11} and 1.03×10^{12} particles/m^3 with a response of approximately 100 ms. Good agreement was found between the developed sensor and a commercially available laser particle counter in measuring ambient PM along a roadside with heavy traffic for about 2 h. The developed sensor proved particularly useful for measuring and detecting particulate air pollution, for number concentration of particles in the range of 10^8 to 10^{12} particles/m^3.

Key words: Aerosol, Particulate Matter, PM2.5, Faraday Cup, Electrometer

INTRODUCTION

Chiang Mai and other major population centers in the north of Thailand have faced serious particulate air pollution problems, especially from December to March for the past several years. Emissions from forest fires, open burning of dried biomass and motor vehicles appear as the dominant sources. This air pollution is harmful to the environment and human health, notably as the particulate matter (PM) in the fraction PM2.5. This fraction refers to particle sizes less than 2.5 μm in aerodynamic diameters, respectively. Recently, concerns over particulate air pollution have emphasized monitoring and measuring these fractions of PM. The US Environmental Protection Agency (EPA) promulgated a new regulation for the mass concentrations of PM2.5. The standards were based on findings from recent health effect studies reporting that PM2.5 could penetrate the alveoli and bypass the upper respiratory tract because they were small enough to allow deposition in places where they could do the most damage [1]. The hazard caused by PM2.5 depends on the chemical composition of the particulate matter and on the site where they deposit within the human respiratory system [2].

To deal with this problem, PM needs to be counted and characterized. For this purpose, PM sensors have been developed to monitor indoor and outdoor aerosols for pollution and to control the pollution processes in industry. The electrostatic PM sensor is a widely used instrument. A typical electrostatic PM sensor consists of two key components, one for PM charging and the other for measuring the electric current on charged PM with an ultra-low current meter or electrometer. The output signal of a electrometer depends strongly on the particle charging technique used. Recent developments on the electrostatic PM sensor were reviewed by Intra and Tippayawong [3]. Many previous studies concerned themselves with measurement of number and surface area concentrations of nanoparticle and fly ash [4-7], ambient ion and aerosol charge measurement [8,9], aerosol integral parameter measurement [10], nanoparticle size distribution measurement [11], engine exhaust particle emission measurement [12,13], and long-term monitoring of ultrafine particles in workplaces [14]. A commercially available instrument, designed to measure net charge on aerosol particles is the TSI Model 3070A Electrical Aerosol Detector [15]. An alternative instrument that can also be used to detect aerosol particles is a condensation particle counter (CPC) using particle growth and optical property [16,17]. These instruments have wide use for detecting and measuring airborne aerosol particles, and provide high-resolution measurements. However, because of the large number of measuring stations distributed in the region, a PM detection system must have a low cost and continuously give fast response measurement of PM2.5 in ambient air. It should also be compact and easy to use, and its maintenance must be possible by relatively low skilled laborers. The ease of moving a sensor should also be considered in measuring and monitoring PM.

Considering this problem, we developed and experimentally tested an inexpensive, fast response, and portable sensor suitable for detection of number concentrations of PM. This system is based on unipolar field and diffusion charging and electrostatic detection of charged aerosol particles. This paper introduces and discusses the detailed description of the operating principle of the system as well as the preliminary experimental testing results of charged aerosol particles and ambient PM in Chiang Mai, Thailand.

PRINCIPLE OF PARTICULATE AIR POLLUTION SENSOR

Fig. 1 shows the schematic diagram of the electrostatic sensor

†To whom correspondence should be addressed.
E-mail: panich_intra@yahoo.com

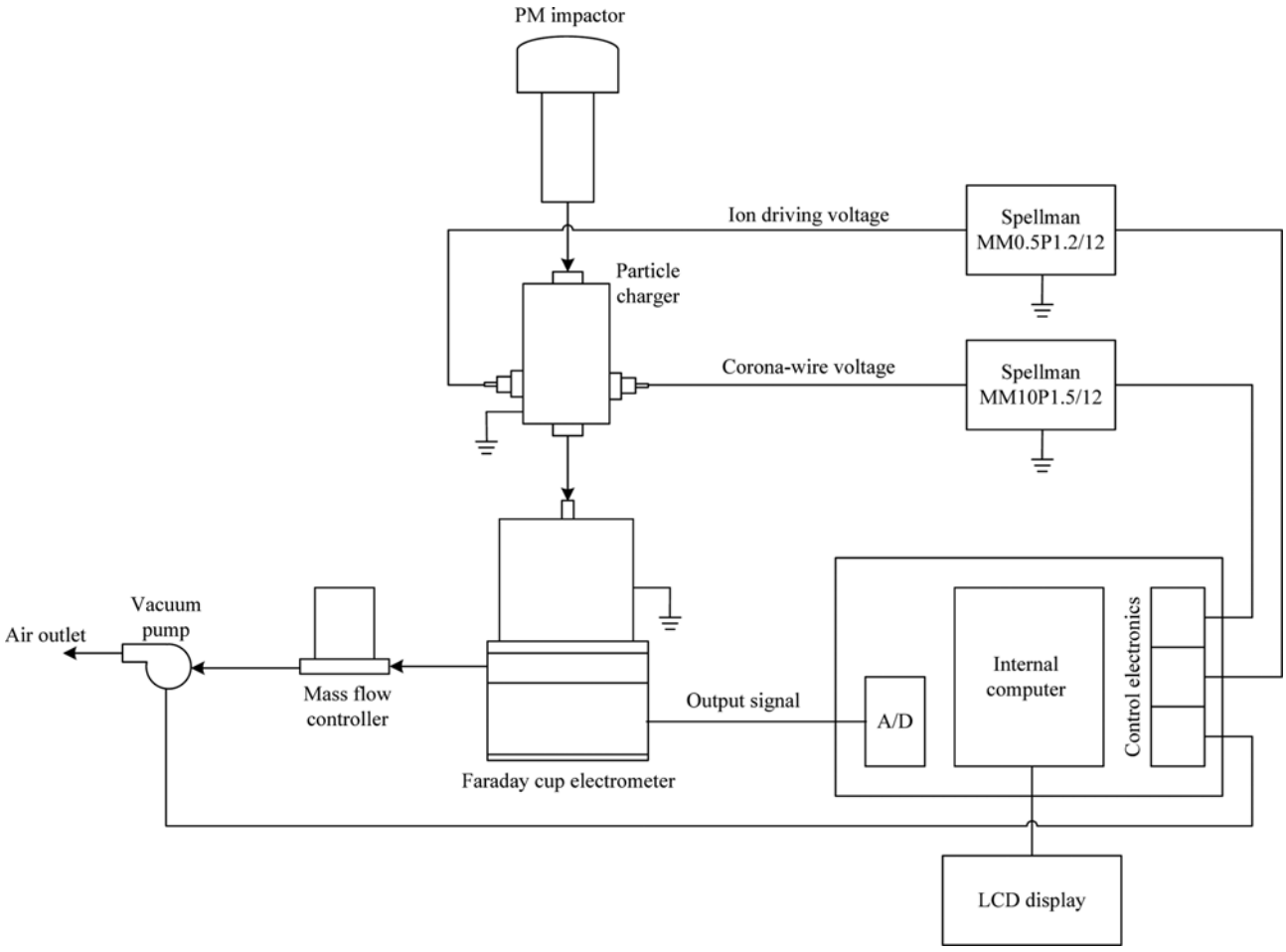

Fig. 1. Schematic diagram of the developed particulate air pollution sensor.

developed in this study. The system consists of a 2.5 micron cut-off diameter impactor, corona diffusion and field charger, Faraday cup, electrometer, flow system, high voltage power supply, and data processing and control system. In this study, the flow system is regulated and controlled by mass flow controllers with a vacuum pump. Sampled PM is first passed through an impactor to remove PM outside the measurement range, particles with diameter larger than 2.5 μm based on their aerodynamic diameter. Sampled PM is then directly introduced into the corona diffusion and field charger to electrostatically charge the particles by attachment of ions produced by the corona discharge inside the charger. The ions are then transported by the electric field and/or by thermal diffusion. PM charging due to the ions transported by electric field is called "field charging". For larger particles (larger than 0.5 μm), field charging is dominant. For smaller particles (smaller than 0.2 μm), thermal diffusion becomes dominant, and "diffusion charging" becomes important [2].

The electrical charges carried by PM then enter into the Faraday cup electrometer and are measured electrically in a Faraday cup electrometer downstream of the charger. The readout of the system shows a relationship between the time and the number concentration

Table 1. Comparison between present sensor and the commercially available sensors

	TSI 3070A	TSI 3010	Intra and Tippayawong [6]	This work
Measurement technique	Electrostatic	Optical	Electrostatic	Electrostatic
Particle size range	10 nm - > 1 μm	10 nm - > 3 μm	10 nm - > 1 μm	10 nm - > 10 μm
Concentration range	2×10^{8}-5×10^{13} particles/m^3	10^{2}-10^{10} particles/m^3	10^{10}-10^{12} particles/m^3	10^{8}-10^{13} particles/m^3
Measurement time	n/a	n/a	<1 s	<250 ms
Current	0.002-400 pA	-	1-500 pA	10 fA-10 pA
Aerosol flow rate	2.5 L/min	2.0 L/min	5.0 L/min	5.0 L/min
Operating temperature range	10-40 ºC	10-35 ºC	10-40 ºC	10-40 ºC
Dimensions	380×280×133 mm	190×220×190 mm	400×200×500 mm	400×570×260 mm
Weight	6.7 kg	5.5 kg	7 kg	5 kg

of PM by the data acquisition and processing system. The developed sensor can also be controlled and data sampled by an external personal computer through a USB/RS-232 port cable. Software running on an external computer was developed based on Visual Basic programming. The software is able to display both size distribution and number concentration. Table 1 shows the comparison between the developed sensor and the commercially available sensors. However, there are differences between the developed sensor and the commercially available sensors: (i) the concept of the developed sensor is based on a compact, inexpensive and portable unit. Overall dimensions and weight are such that it is easy to handle and move around; (ii) in the case of PM10 and PM2.5, the developed sensor employs unipolar corona diffusion and field charger for charging aerosol particles in the size range smaller than 2.5 and 10 μm; and (iii) the mass, shape, size, and chemical composition of collected aerosol on the filter inside the Faraday cup can be further analyzed. The following section gives a detailed description of the main components of the fast response particulate air pollution sensor.

COMPONENT DESCRIPTION

1. Impactor

The impactor was designed as a size selective inlet for classifying airborne particulate matter with sizes smaller than 2.5 μm based on their aerodynamic diameter. It is similar to the typical round jet impactor configuration used in Marple and Willeke [18], and Intra et al. [19]. Schematic diagram of the impactor is shown in Fig. 2. The acceleration nozzle and the impaction plate are made of PTFE (polytetrafluoroethylene) because of its good electrical properties and it is lightweight and inexpensive. Unfortunately, charge accumulation on this non-conductive surface would likely result in particle losses by electrostatic deposition. However, this loss is expected to be small because of the short exposure time. The particulate flow could vary in the 5-15 L/min range. The acceleration nozzle diameter is 2.8 mm. The distance from the nozzle to the impaction plate is 10 mm. The impaction plate deflects the flow streamlines to a 90° bend. Therefore, the particle collection efficiency, η, of the impactor can be estimated from [19]

$$\eta(d_p) = \frac{1}{1+(d_{50}/d_p)^{2s}} \tag{1}$$

where d_{50} is the particle cut-off diameter at 50% collection efficiency, d_p is the particle diameter and s is the parameter affecting the steepness of the collection efficiency curve. For an ideal impactor without wall losses, s=1 is arbitrarily assumed for the steepness of the collection efficiency curve [19]. The particle cut-off diameter at 50% collection efficiency can be calculated by the following equation:

$$d_{50} = \sqrt{\frac{9\rho D^2 Stk_{50}}{\rho_p Re C_c}}, \tag{2}$$

where ρ is the gas density, D is the acceleration nozzle diameter, Stk_{50} is the Stokes number of the particle cut-off diameter at 50% collection efficiency (for a round jet impactor, Stk_{50} is 0.24 [2]), ρ_p is the particle density, Re is the Reynolds number and C_c is the Cunningham slip correction factor. The expression for Reynolds number is given by

$$Re = \frac{\rho V_0 D}{\mu} = \frac{4\rho Q}{\pi \mu D} \tag{3}$$

where V_0 is the average velocity, Q is the aerosol flow rate and μ is the gas viscosity. The average velocity within the round jet can be calculated by

$$V_0 = \frac{4Q}{\pi D^2} \tag{4}$$

Based on the Stokes number equation for a round jet impactor [18], Fig. 3 shows the variation of the theoretical collection efficiency curves as a function of particle size at aerosol flow rates. The calculations were done for an acceleration nozzle diameter of 2.8 mm, a Reynolds number of 1.56×10^8, 3.11×10^8 and 4.67×10^8 corresponding to aerosol flow rates of 5, 10 and 15 L/min, a particle size range from 0.1 to 100 μm, air density of 1.225 kg/m^3, viscosity of 1.7894×10^{-5} kg/m/s and temperature of 294 K. It was shown that the cut-off diameter decreased as the aerosol flow rate increased. For the performance of the impactor, flow rates of 5 and 15 L/min gave cut-off diameters of about 2.5 and 1.5 μm, respectively. It was expected that the collection efficiency increased with flow rate because of the higher inertial force acting on the particles at higher velocities. The collected particles on the impaction plate and downstream of the impactor were also analyzed by scanning electron microscope (SEM). The SEM results agreed well with the theoretical predictions as shown in Fig. 3 [19].

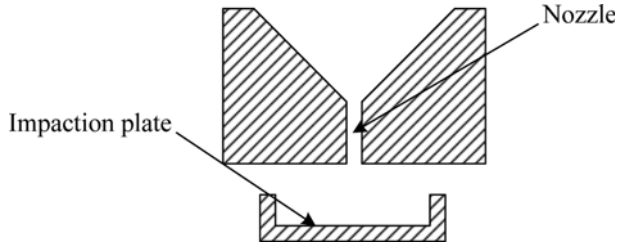

Fig. 2. Schematic diagram of the impactor.

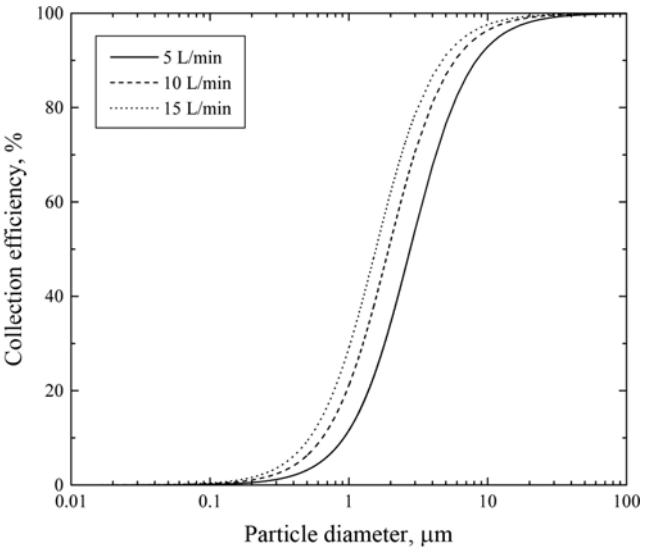

Fig. 3. Variation of theoretical collection efficiency with particle diameter of the impactor.

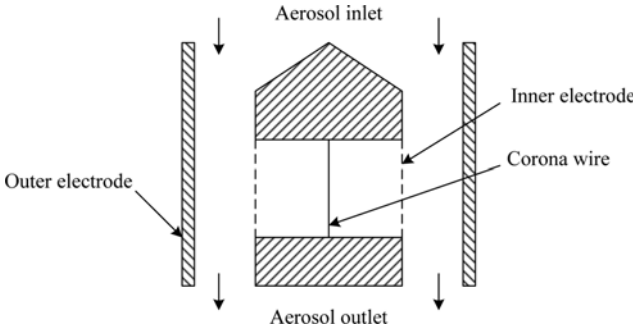

Fig. 4. Schematic diagram of the corona diffusion and field charger.

2. Corona Diffusion and Field Charger

Fig. 4 shows a schematic diagram of the corona diffusion and field charger. The prototype charger is 126 mm in length and 67 mm in diameter. It consists of two concentric cylinders with a corona-wire (20 mm in length and 0.3 mm in diameter) placed along the axis of the cylinders. The corona-wire and inner and outer cylinders were fabricated of stainless steel, and were polished to an extremely fine surface finish to avoid distortion of the electrical field from small surface scratches and imperfections. Stainless steel was used because it is electrically conductive, inert, corrosion resistant and very hard, and therefore resistant to scratching. The inner and the outer radii of the annular charging zone were 17 mm and 30 mm. The electrical insulation was provided by a Delrin® spacer between the inner and outer cylinders. A DC high voltage was applied to the corona-wire to produce a corona discharge and the generated ions migrated toward the inner cylinder due to the high electric field in the region. To allow ions to flow in the charging zone, a section of the inner cylinder was made out of a perforated (2.5 mm diameter) cylindrical tube. The width of the perforated screen opening on the inner cylinder is 20 mm. The ion-driving DC voltage applied on the inner cylinder forces the ions through the perforated screen openings on the inner cylinder to the charging zone, while the outer cylinder is connected to ground. This ion-driving voltage can regulate the ion current flow through the perforated screen. In the past, AC electric fields have been used to regulate the ion current flow through the perforated screen into the charging zone and shown to reduce charged particle losses inside charging zone and higher charging efficiencies [20]. However, AC electric fields were reported by numerous works to promote agglomeration of charged particles, which caused a reduction in the number concentration of particles by approximately 30% in the 0.3-2 μm size range [21]. The present DC charger is reported to have about 14% of charged 10 nm particles lost inside the charging zone [22].

In the charging zone, the PM is charged electrically through collision with the ions. Thus, the mean charge per particle, n_p, caused by the diffusion and field charging in a time period, t, by a particle diameter is approximately determined by the theory of White [2]

$$n_p = \frac{d_p kT}{2K_E e^2}\ln\left|1+\frac{\pi K_E d_p \bar{c}_i e^2 n_i t}{2kT}\right| + \left|1+2\frac{\varepsilon-1}{\varepsilon+2}\right|\left|\frac{E_{ch} d_p^2}{4K_E e}\right|\left|\frac{\pi K_E e Z_i n_i t}{1+\pi K_E e Z_i n_i t}\right| \quad (5)$$

where k is the Boltzmann's constant (1.380658×10^{-23} J/K), T is the operating temperature, K_E is the Coulomb constant, ε_0 is the vacuum permittivity (8.854×10^{-12} F/m), $\bar{c}_i$ the mean thermal speed of the ions, e is the value of elementary charge on an electron (1.61×10^{-19} C), ε is the particle dielectric constant, E_{ch} is the average electric field in the charging zones, Z_i is the electrical mobility of ions, n_i is the ion number concentration, and t is the time of exposure of the particles to the ions. In the present charger, the product of the ion concentration and charging time, $n_i t$, can be calculated when the charging currents, I_{ch}, the corona voltages, V, are known, and is given by

$$n_i t = \frac{I_{ch}}{2\pi r e Z_i}\left|\frac{(r_2^2 - r_1^2)}{Q_a}\right| \quad (6)$$

where r_1 and r_2 are the radius of the inner and outer electrode, respectively, and Q_a is the aerosol flow rate. In this charger, the ion concentration was about 1.47×10^{14} ions/m^3 for corona voltage of 10 kV and the charging times were in the range of about 0.4-2 s for aerosol flow rate between 1 and 5 L/min.

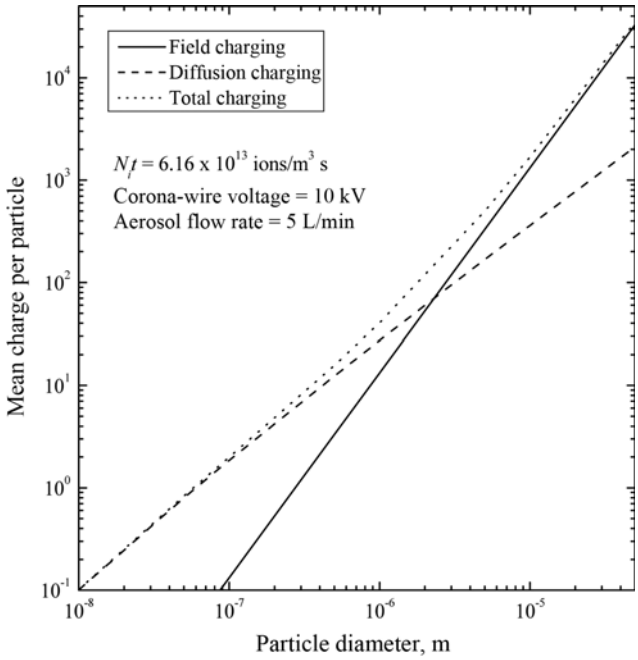

Fig. 5. Mean charge per particle as a function of the particle diameter of the charger.

Fig. 5 shows the theoretical prediction of the mean charge per particle of the corona diffusion and field charger as a function of particle diameter from 0.1 to 100 μm. We estimated the mean charge per particle from White's theory [2]. For a particle diameter less than 1 μm, the electric field in the charger had a negligible effect on the charging process. It was shown that the mean charge per particle increased with particle diameter. Note that, for larger than 10^{13} s/m^3, White's charging equation is accurate to particles with diameters from 0.07 to 1.5 μm for diffusion charging and particles with diameters from 0.05 to 40 μm for field and diffusion charging at standard conditions. Diffusion charging is the dominant mechanism for particles with diameters less than 0.1 μm, even in the presence of an electric field.

3. Faraday Cup

This device is an open-ended cup with a filter to collect the charges (Fig. 6). The present device consists of a Faraday housing, filter holder, high efficiency particulate air (HEPA) filter, Teflon® insulator

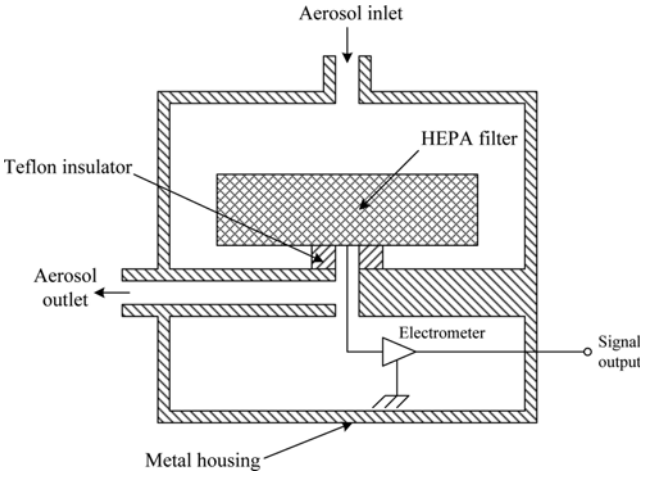

Fig. 6. Schematic diagram of the Faraday cup.

and electrometer housing. To completely shield the filter collecting the charged aerosol, the external housing is made of stainless steel, and the filter holder is electrically isolated from the external housing with a Teflon® insulator (volume resistivity exceeding 10^{18} Ωcm). The filter holder is made of a stainless steel tube with a tapered end with a diameter of 47 mm. The conductive filter is placed in the filter holder on the top of a rigid stainless-steel net. The Faraday cup helps eliminate electrical noise from the measurement of ultra-low currents produced by the charges collected on the internal filter. Because the material of the filter holder is a conductor, charges collected in the filter can move to the electrometer circuit through the connecting electrode without delay. The connecting electrode is electrically connected to the filter holder and the input of the electrometer circuit located inside the electrometer housing. The signal current, I_p, of collected charges on the filter in the Faraday cup as a function of ion number concentration can be calculated by [6]

$$I_p = N_p e Q_a \tag{7}$$

where N_p is the total number concentration of PM. In addition, the collected aerosols on the HEPA filter inside the Faraday cup can be further analyzed for their mass, shape, size, and chemical composition.

4. Electrometer Circuit

Fig. 7 shows the schematic diagram of the electrometer circuit. The electrometer circuit is a simple current-to-voltage converter,

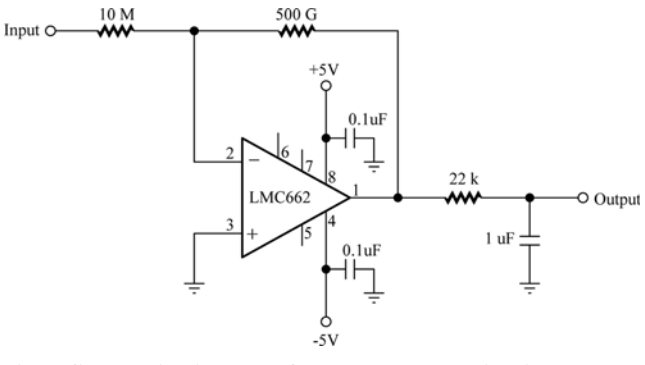

Fig. 7. Schematic diagram of the electrometer circuit.

where the voltage drop caused by a current flowing through a resistor is measured. A negative feedback amplifier was used in this study. In this circuit, the input current, I_i, flows through the feedback resistor, R_f. The low offset current of the amplifier changes the current by a negligible amount. Therefore, the amplifier output voltage, V_o, can be calculated as follows:

$$V_o = -I_i R_f \tag{8}$$

The output voltage is a measure of the input current, and the overall sensitivity is determined by the feedback resistor consisting of a 500 GΩ resistor with a percent error of 10% (OHMITE model RX-1M5009KE). To avoid expensive construction, commercially-available low-cost monolithic operational amplifiers were used (LMC662). These were designed for low current measurement and featured an ultra-low input bias current (2 fA maximum) and low offset voltage drift, typically about 1.3 μV/°C. It required a ±5 V power supply capable of providing 100 mA. Other components in this circuit were primarily for input protection and RC low-pass filtering. This reduced high-frequency noise and prevented oscillations of the amplifier output. The cut-off frequency and the time constant of this circuit were typically 4.82 Hz and 0.033 s. This circuit gave an output voltage of 5 mV per 10 fA of input signal current. Its output voltage, in the range of 5 mV to 5 V, linearly translated into current measurements of 10 fA to 10 pA. The sensitivity of the electrometer was limited by the range of particle concentration to be detected by the sensor. In this sensor, as a rough estimate by Eq. (7) at the worst predicted conditions, the signal current levels in the range of about 10 fA will correspond to about 7.5×10^7 particles/m^3.

A high-impedance current source was used to calibrate the prototype electrometer circuit in this study. The schematic diagram of the experimental setup for calibrating the electrometer circuit is shown in Fig. 8. The high-impedance current source consisted of a standard resistor of 500 GΩ with a percent error of 10% (OHMITE model RX-1M5009KE) and an adjustable voltage source in the range between 0-5 V (built-in voltage source of the Keithley 6517A and a resolution of 5 mV). The output current of this circuit could simply be calculated from Ohm's law:

$$I = \frac{V_s}{R_{cal}} \tag{9}$$

where V_s is the source voltage, and R_{cal} is the standard resistance. The range of the output current was from 10 fA to 10 pA. Fig. 9

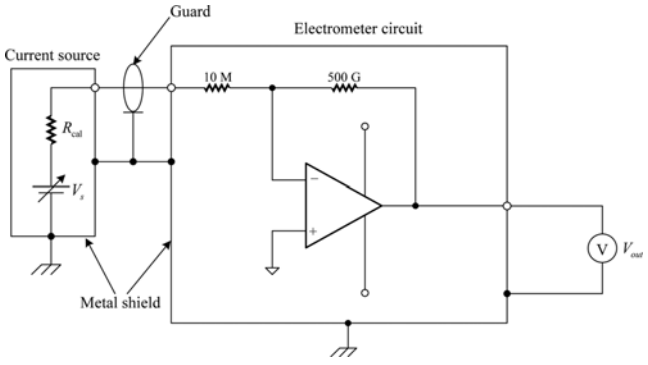

Fig. 8. Schematic diagram of the experimental setup for calibrating the electrometer circuit.

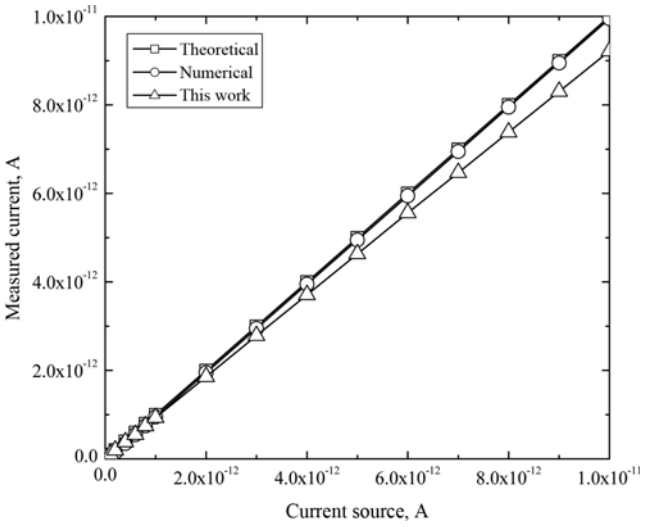

Fig. 9. Comparison between measured and predicted currents of the electrometer.

shows the comparison between measured and predicted currents for the electrometer circuit. In this study, the prototype electrometer circuit was calibrated with a high-impedance current source and compared with theoretical and numerical predictions. Good agreement was found for the comparison, i.e., the average differences were within 7.4% and the measured current ratio was in the range of 1.07-1.09.

5. Flow System

The aerosol flow was regulated and controlled by thermal mass flow meters and controllers with a vacuum pump; a commercial gas mass flow controller, Dwyer model GFC-1111, was used. It was operated at flow rates that ranged from 0 to 15 *l*/min. The vacuum pump, an oil-less diaphragm vacuum pump, GAST model 15D1150/1190, was used to deliver the aerosol flow into the system. It had a maximum pressure of 20 psi, and an open volume rate of 7 L/min. Polyethylene tubing (5 mm I.D.×8 mm O.D.) was used for the connecting tube system.

6. High Voltage Power Supply

A DC high voltage power supply was used to maintain the corona-wire and ion-driving voltages in the charger. Commercial high voltage power supplies, Spellman model MM10P1.5/12 and MM0.5P1.5/12, were used. The maximum output voltages of both MM10P1.5/12 and MM0.5P1.5/12 were 10 kV and 500 V, respectively, with a maximum load power of 1.5 W and a ripple voltage of 200 $V_{p\text{-}p}$. In addition, the output voltages of both power supplies could be controlled by varying the input voltage in the range of 0 to 12 V corresponding to the output voltage in the range of 0 to 10 kV for MM10P1.5/12 and 0 to 500 V for MM0.5P1.5/12, respectively.

7. Data Processing and Control

The main component, the Microchip PIC18F46K80 microcontroller, was equipped with 64 Kbytes on-chip flash program memory and 64 MHz of processing speed. A build-in 12-Bit A/D converter converted all analog outputs from the electrometer circuit into digital signals fed to the microcontroller. To display the measurement of the sensors and the current time, an LCD module was connected to the microcontroller. The data logger allowed browsing through the recorded data and changing the sampling interval. Data stored in the memory could be accessed directly with an external computer through a USB connection. The graphical user interface software was developed using Visual Basic. The software allowed complete or partial downloading of data from memory; it also enabled changing sampling parameters such as date, time and sampling interval. The data could be plotted with the built-in graph plotter or exported to Excel for further analysis.

CHARGED AEROSOL MEASUREMENT AND FIELD TESTING

The developed sensor was experimentally evaluated with a combustion aerosol generator. The experimental setup, shown in Fig.

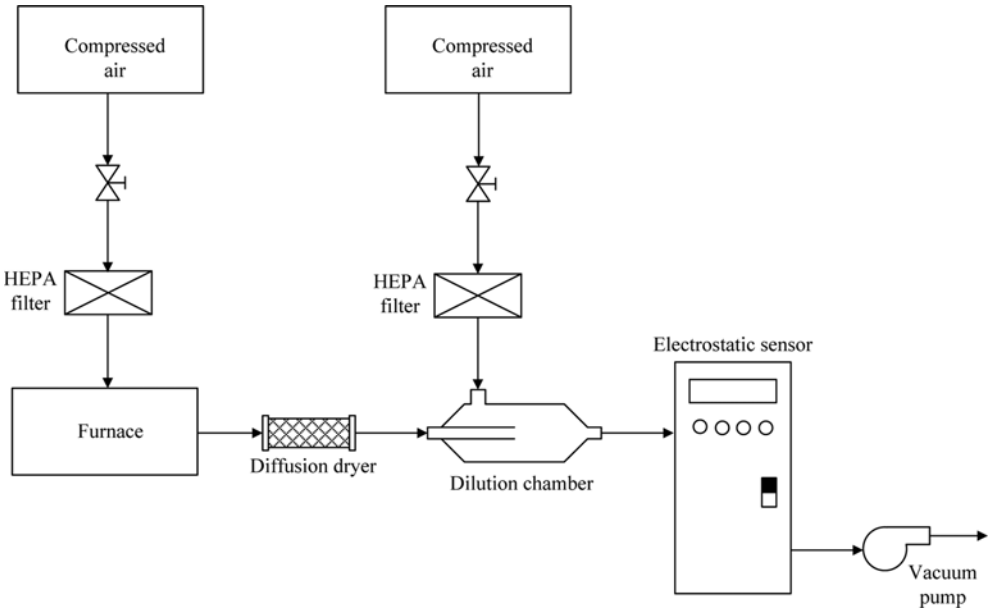

Fig. 10. Schematic diagram of the experimental setup for charged aerosol measurement of the developed sensor.

10, consisted of a combustion aerosol generator (CAG), a dryer, a dilution chamber, a HEPA filter, and a vacuum pump. The CAG was used to generate polydisperse, carbonaceous diffusion flame aerosols [23]. The particle size distribution of the CAG was in the range of approximately 50 nm to several micron-sized with particle number concentrations larger than 10^{10} particles/m^3, which was measured by an electrical mobility spectrometer (EMS) [24]. For the measurement, the vacuum pump was switched on and the aerosol sample was sucked into the sensor using an isokinetic sampling system. The aerosol particles were first dried with the dryer and before they entered the system, the particles were diluted and mixed with clean air, which had been filtered through a HEPA filter in the mixing chamber. The sensor was operated at aerosol flow rates in the range of 5.0 L/min. For each set of operating conditions, measurements were repeated at least three times. Table 2 shows the operating conditions used for this experiment. The time variation of the measured number concentration of charge aerosol particles from the Faraday cup electrometer at an aerosol flow rate of 5 L/min with a time of measurement of 15 min is given in Fig. 11. It shows that the measured number concentrations of charge aerosol particles were in the range of about 2.02×10^{11} to 1.03×10^{12} particle/m^3 with the time response of approximately 100 ms.

For ambient aerosol particle measurements, the performance of the developed sensor was evaluated simultaneously with a currently available IQAir laser particle counter, model ParticleScan, at ambient conditions. The measurement location was on a roadside of a Chiang Mai highway with heavy traffic for about 2 h during 27-28 August 2012. Fig. 12 shows the comparison between the developed sensor and the ParticleScan. There was good agreement for the comparative study. The measured number concentration of ambient aerosol particles for both sensors was in the range of approximately 10^8 to 10^9 particles/m^3. As shown in Table 3, the maximum particle concentrations were about 6.70×10^8 and 1.44×10^9 particles/m^3, minimum particle concentrations were about 9.98×10^7 and 5.17×10^7 particles/m^3, and average particle concentrations were about 1.84×10^8 and 2.25×10^8 particles/m^3 for the ParticleScan and the developed sensor, respectively. The average difference of particle concentrations between the ParticleScan and developed sensor was about 4.04×10^7 particles/m^3. Continuous operation of the sensor did not

Table 2. The operating conditions for combustion aerosol measurement

Operating conditions	Values
Particle size range	Smaller than 2.5 μm
Particle concentration range	Larger than 10^{10} particles/m^3
Corona-wire voltage	10 kV
Ion-driving voltage	500 V
Aerosol flow rate	5 L/min
Operating pressure	1 atm
Operating temperature	30 °C

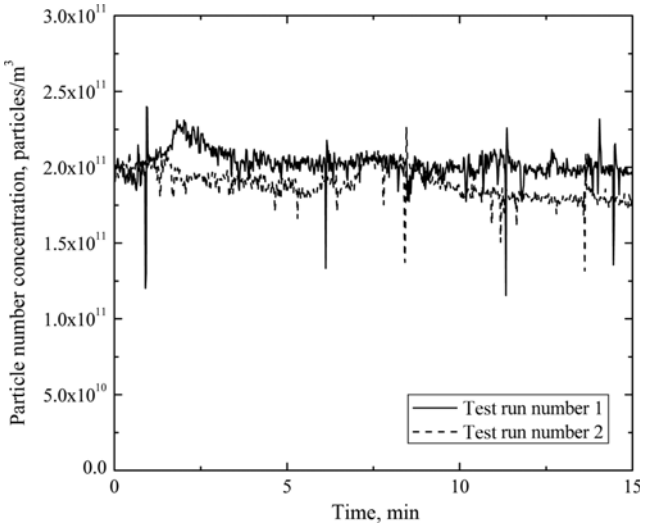

Fig. 11. Temporal variation of measured number concentration of the combustion aerosol.

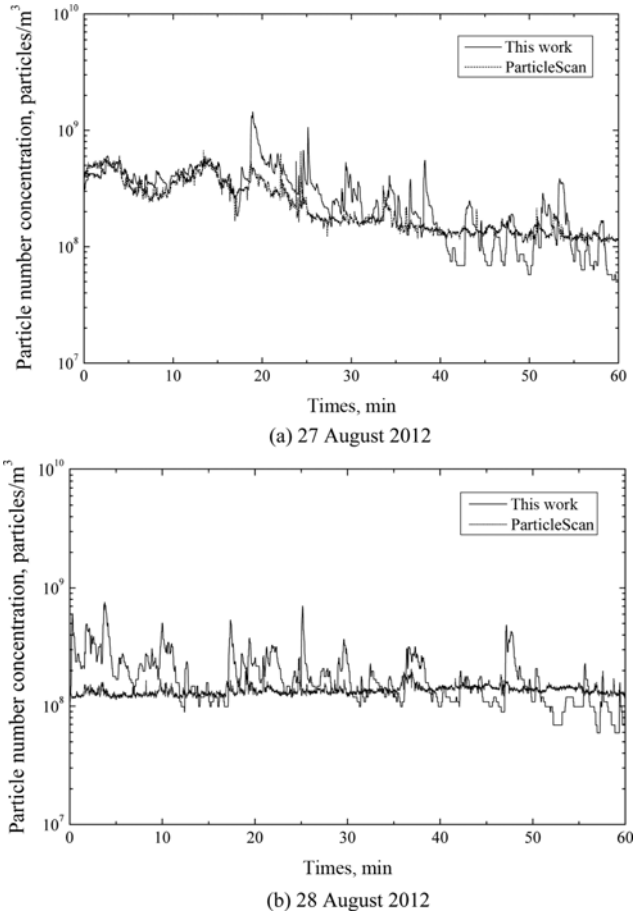

Fig. 12. Comparison between the developed sensor and the ParticleScan at ambient conditions along a roadside with heavy traffic.

Table 3. Comparison between the developed sensor and the ParticleScan at ambient air conditions in Chiang Mai, Thailand highway with heavy traffic for about 2 hours

Particle number concentration	ParticleScan (particles/m^3)	This work (particles/m^3)	Difference (particles/m^3)
Maximum	6.70×10^8	1.44×10^9	7.70×10^8
Minimum	9.98×10^7	5.17×10^7	4.81×10^7
Average	1.84×10^8	2.25×10^8	4.04×10^7

result in any measurable changes in the performance of the sensor. No visible deposits could be observed. This indicated that the maintenance interval (for calibration, cleaning and etc.) may be greater than 50 h of operation at relatively high concentrations of particles.

CONCLUSION

A particulate air pollution sensor for measuring and detecting particle number has been developed and experimentally evaluated. The measuring method was based on unipolar corona charging and electrostatic detection of charged aerosol particles. Presented here are the detailed description and the operating principle of the system. The sensor was experimentally evaluated by using combustion aerosol with sizes in the range of approximately 50 nm to several microns and number concentrations of approximately 10^{10}-10^{14} particles/m^3. Measurements of the aerosol charges were very promising. It was demonstrated that the sensor can be used in detecting particle number concentrations in the range of 2.02×10^{11} and 1.03×10^{12} particles/m^3 with a resolution of approximately 100 ms. Performance of the developed sensor was evaluated simultaneously with a commercially available laser particle counter on a roadside with heavy traffic for about 2 h. Good agreement was found from the comparison. This showed that an inexpensive sensor proved to be particularly useful for measuring and detecting particulate air pollution.

RECOMMENDATIONS FOR FUTURE WORK

- For most impactors, the cut-point curve is 50% collection efficiency. One of the principal limitations of the inertial impaction method is that a significant fraction of the particles greater than the cut-off point diameter (50% is from particle larger than the cut-off point) pass through the impactor. Therefore, further research should focus on the effect of a fraction of the particles larger than the 50% cut-off point diameter on the overall performance of the sensor.
- The actual charging performance of the charger should be investigated with monodisperse particles to determine the equilibrium unipolar charge distribution of the multiply charged particles at the outlet of the charger. Use of different aerosol generators that cover the greater size range will give a better understanding on the charging performance.
- Calibration and comparison of the instrument with other particle measuring devices should be explored further.

ACKNOWLEDGEMENTS

The authors wish to express their gratitude to the Hands-on Research and Development Project, Rajamangala University of Technology Lanna, Thailand, contract no. UR2L-002. The authors also wish to thank Dr. Rainer Zawadzki for the valuable contribution during the preparation of this article.

REFERENCES

1. EPA, *National Ambient Air Quality Standards for Particulate Matter*, Final Rule, Federal Register, 62, 38651(1997).
2. W. C. Hinds, *Aerosol technology*, John Wiley & Sons, New York, USA (1999).
3. P. Intra and N. Tippayawong, *Maejo Int. J. Sci. Technol*., **1**, 120 (2007).
4. T. Johnson, S. Kaufman and A. Medved, *6th Int. ETH Conference Nanoparticle Measurement*, Zurich, Switzerland, 19-21 August (2002).
5. J. Wei, *Development of a method for measuring surface area concentration of ultrafine particles*, D. Eng. Thesis, University of Duisburg-Essen, Germany (2007).
6. P. Intra and N. Tippayawong, *J. Japan Soc. Appl. Electromagnet. Mech*., **17**, s17 (2009).
7. J. K. Kim and S. C. Kim, *Korean J. Chem. Eng*., **18**, 531 (2001).
8. M. Murtomaa, P. Pekkala, T. Kalliohaka and J. Paasi, *J. Electrostat*., **63**, 571 (2005).
9. F. O. J-Fatokun, L. Morawska, M. Jamriska and E. R. Jayaratne, *Atmos. Environ*., **42**, 8827 (2008).
10. L. Li, D. R. Chen and P. J. Tsai, *J. Electrostat*., **67**, 765 (2009).
11. L. Li, D. R. Chen and P. J. Tsai, *J. Nanopart. Res*., **11**, 111 (2009).
12. L. Ntziachristos, B. Giechaskiel, J. Ristimaki and J. Keskinen, *J. Aerosol Sci*., **35**(8), 943 (2004).
13. A. Rostedt, M. Marjamaki, J. Yli-Ojanpera, J. Keskinen, K. Janka, V. Nienela and A. Ukkonen, *Aerosol Air Qual. Res*., **9**, 470 (2009).
14. T. Lanki, J. Tikkanen, K. Janka, P. Taimisto and M. Lehtimaki, *J. Physics Conf. Series*, **304**, 012013 (2011).
15. TSI Incorporated, Instruction Manual for Electrical Aerosol Detector Model 3070A, Minnesota, USA (2002).
16. J. K. Agrawal and G. J. Sem, *J. Aerosol Sci*., **11**, 343 (1980).
17. TSI Incorporated, Instruction Manual for Condensation Particle Counter Model 3010, Minnesota, USA (2002).
18. V. A. Marple and K. Willeke, *Atmos. Environ*., **10**, 891 (1976).
19. P. Intra, A. Yawootti, U. Vinitketkumnuen and N. Tippayawong, *Korean J. Chem. Eng*., **29**, 1044 (2012).
20. P. Intra and N. Tippayawong, *Aerosol Air Qual. Res*., **11**, 187 (2011).
21. M. Kobashi, *Particle agglomeration induced by alternating electric fields*, Ph.D. Thesis, Stanford University (1979).
22. P. Intra, *J. Electrostat*., **70**, 136 (2012).
23. T. G. Cleary, G. W. Mulholland, L. K. Ives, R. A. Fletcher and J. W. Gentry, *Aerosol Sci. Technol*., **16**, 166 (1992).
24. P. Intra and N. Tippayawong, *Korean J. Chem. Eng*., **26**, 1770 (2009).